Electric Power Systems Research 200 (2021) 107412

Contents lists available at ScienceDirect

Electric Power Systems Research

journal homepage: www.elsevier.com/locate/epsr

Modified repetitive control based on comb filters for harmonics control in grid-connected applications

Tomasz Chmielewski [a,*], Wojciech Jarzyna [a], Dariusz Zieliński [a], K. Gopakumar [b], Magdalena Chmielewska [c]

[a] Department of Electrical Drives and Machines, Lublin University of Technology, 20-618 Lublin, Nadbystrzycka 38A, Poland
[b] Department of Electronic Systems Engineering, Indian Institute of Science, Bangalore 560012, India
[c] Department of Computer Science, Lublin University of Technology, 20-618 Lublin, Nadbystrzycka 36B, Poland

ARTICLE INFO

Keywords:
Comb filters
Harmonic distortion
Current control
Repetitive control

ABSTRACT

Power quality plays an important role in the operation of grid-connected inverters. The injected current should have a minimum harmonic content in order to comply with the local grid codes. This can be challenging due to the fact that the grid voltage can also be distorted. This paper presents the modified repetitive control method for three-phase grid-connected inverters by means of a digital comb filter application. The proposed method provides multiple harmonics compensation, simple implementation and design. It consists in complementing the Proportional-Resonant (PR) control with an appropriately tuned comb filter, which results in mitigation of the output current harmonics and reduced THD. Two types of comb filters have been proposed as a harmonic compensator, namely feedback and feedforward structures. The compensator included an additional FIR low-pass filter for increased robustness. Regardless of the structure chosen the solution is targeted at simplicity of analysis, design and implementation. Furthermore, the compensator based on the feedforward comb filter is casual, hence its implementation on the digital microprocessors is greatly facilitated. The proposed two-stage design of the control loop ensures the stability even in the case of additional poles being introduced by the feedback comb filter. Investigation on frequency variations impact is also included. The research was conducted by means of the following IT solutions: data workflow management environment, code design and generation (Matlab), and user interface design (ControlDesk). The experimental results have demonstrated the effectiveness of the proposed solution for a grid-connected converter operating in a network with distorted supply voltage.

1. Introduction

Harmonics in the power system occur due to the presence of nonlinear loads such as power transformers, arc furnaces, welders, reactors or switch-mode converters. Regardless of the harmonics emission source, their presence will be manifested in the supply voltage due to the fact that the power systems have a limited short-circuit capacity, i.e. there is a series impedance [1]. The content of harmonics in inverter current can be additionally increased by the presence of grid voltage distortion. Therefore, the impact on the voltage quality of the inverter itself should be minimised to prevent further voltage distortion. Moreover, in the case of grid applications such as renewables integration, the local grid codes can strictly outline the permissible current harmonics injection and when exceeded, does not grant the permission of operation. This is due to the fact that an increasing number of nonlinear power sources and load may lead to power quality issues, resulting in higher losses (both conduction and iron core portions) and heating, which may adversely affect the lifespan of system components due to e.g. insulation degradation, transformer elements overload, distorted operation of utility equipment, etc. When it comes to grid-connected inverter operation, the harmonics emission can be decreased with appropriate control, modulation or topology [2–5]. The topology of the inverter plays an important role in the possible reduction of current or voltage harmonics. An increasing number of output voltage levels tends to decrease the harmonics content both in current and voltage. The numbers of output voltage levels can be increased either by means of bridge topology, e.g. Neutral Point Clamped (NPC) inverter or the introduction of modular structure (Modular Multi-Level Converter, MMC). In the case control structures impact on the harmonics, the application of selective harmonics compensation algorithm can be applied for its reduction. Such an

* Corresponding author.
E-mail address: tomasz.chmielewski@pollub.edu.pl (T. Chmielewski).

https://doi.org/10.1016/j.epsr.2021.107412
Received 31 May 2020; Received in revised form 12 December 2020; Accepted 2 June 2021
Available online 1 August 2021

approach may concern the voltage control (e.g. islanded microgrids, shore-to-ship supply) or current control loops when the inverter operates in a grid-connected mode in the presence of background voltage harmonics in the supply voltage. When the inverter is operating in the voltage mode the harmonics can be controlled effectively with modulation by the selection of an optimal pattern of gating pulses. This topic was discussed in [6]. In the second case when the grid-connected inverter is in current or power control mode the output current can be contaminated with harmonics of the same order as in voltage. In order to prevent this phenomenon, a harmonics compensation control can be used. Harmonic compensation is a topic widely addressed in the literature [7–12]. In the case of linear controllers harmonic compensation can be implemented either in Synchronous Rotating Reference Frame (dq0) or in Stationary Reference Frame ($\alpha\beta 0$) [13]. In stationary reference frame, the cascaded resonant controllers tuned at a selected harmonic are typically used. Synchronous rotating reference frame based algorithms require multiple coordinate transformations and symmetrical components decomposition [8, 14]. Conventional repetitive controllers (CRC) have also been demonstrated effective for current or voltage harmonics control [15–20]. CRC can be used as direct regulators or cascaded with typical feedback controllers as a plug-in, series structure [19–22]. In this paper, only a paralleling with the main control is considered in order to account for a modular and simple design.

The solution proposed in this paper is based on the modified repetitive control seen as comb filters. The compensator is paralleled with typical PR control, both operating in a stationary reference frame. Two different structures of digital comb filter are proposed for control of odd-order harmonics in the inverter output current. The proposed method can provide multiple harmonics compensation basing only on two additional filters, which greatly reduced the control loop complexity. The compensator based on filter block that has a clear notation in the discrete-time domain is additionally less complex for digital implementation. The distinct difference between CRC and the proposed approach is in a simplified transfer function with normalization factors for simplification of the control loop design procedure and a better understanding of the compensation level. Moreover, it allows using both FIR and IIR forms of the compensator.

2. Comb filter – modified structure and properties applicable for harmonics control

The comb filters have analysed herein can have either finite or infinite impulse response. The transfer functions of two types of comb filter are presented in (1)-(3).

$$G_{FB} = K_n \cdot \frac{1}{1+gz^{-M}} = \left(\frac{1}{1-|g|}\right)^{-1} \cdot \frac{1}{1+gz^{-M}} \tag{1}$$

$$G_{FF} = K_n \cdot \left(1+gz^{-M}\right) = \frac{1}{1+|g|} \cdot \left(1+gz^{-M}\right) \tag{2}$$

$$M = \frac{f_s}{f_o} \tag{3}$$

where M – is the delay window, g – damping coefficient, K_n – gain normalization coefficient, f_s – sampling frequency, f_0 – resonant frequency.

The above transfer function structure can be visualized as depicted in Fig. 1. Compared to CRC it is missing the internal filter and derivative term in the numerator [17, 21]. Moreover, the normalization coefficient K_n has been introduced here that ensures zero gain of the filter. It effectively means that with unity compensator gain, regardless of the structure, the compensation level is low and only the filtered error is feedforwarded. The digital implementation of the feedback and feedforward comb filters can be done according to (1) and (2) respectively, with delay line length equal to M as in (3). The magnitude and phase characteristics of the feedback and feedforward comb filters for different values of g and with K_n included are depicted in Fig. 3. What is noteworthy, the filter does not introduce the phase shift at the resonance frequencies. The comb filters are used in power electronics control e.g. for filters control and grid synchronization [23, 24]. There are also applications where comb filter is built using individual components [25].

The g damping is the crucial parameter to the comb filter properties. Not only can it be used to adjust the resonant peaks value but also provides the numerical stability for the feedback structure. This is done by shifting the poles of the system inside the unity circle as presented in Fig. 2. Additional stability improvements are presented further in this paper. Due to its characteristics, the comb filter is able to attenuate or magnify evenly distributed harmonics. This feature can be used for harmonics control in the VOC operating in stationary reference frame as it is explained further in this paper.

In order to provide damping of even order harmonics and DC component (Fig. 3) the following g coefficient sign and parameters to calculate the delay line M should be used:

- feedback comb filter $0 > g > 1$ and f_0 = two times grid nominal frequency,
- feedforward comb filter $-1 < g < 0$ and f_0 = two times grid nominal frequency.

3. Proposed control algorithm with multiple harmonics compensation

A. Overall description

The proposed structure applicable for grid-connected inverters is based on the voltage oriented control (VOC) operating in a stationary reference frame (Fig. 4). The current control loop is equipped with PR controllers [26]. The proposed harmonic compensator is connected in parallel with the main current control loop. It comprises comb filter, compensator gain K_{HC} and casual FIR low-pass filter $G_f(z)$ in the form described in (6). Discrete transmittance $G_{PR}(z)$ expresses the proportional-resonant component described by (5), derived from the continuous time domain transfer function (4). This *low-pass* filter in series with the comb one is used to increase system robustness and facilitate the control loop design.

$$G_{PR}(s)_{\alpha\beta} \approx \begin{bmatrix} k_p + \dfrac{2k_r\omega_c s}{s^2+2\omega_c s+\omega^2} & 0 \\ 0 & k_p + \dfrac{2k_r\omega_c s}{s^2+2\omega_c s+\omega^2} \end{bmatrix} \tag{4}$$

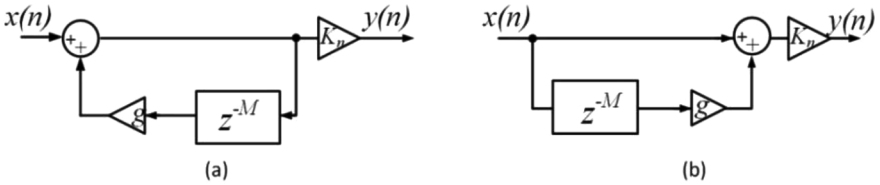

Fig. 1. Block diagram of (a) feedback form and (b) feedforward form of a comb filter with introduced K_n gain normalization coefficient.

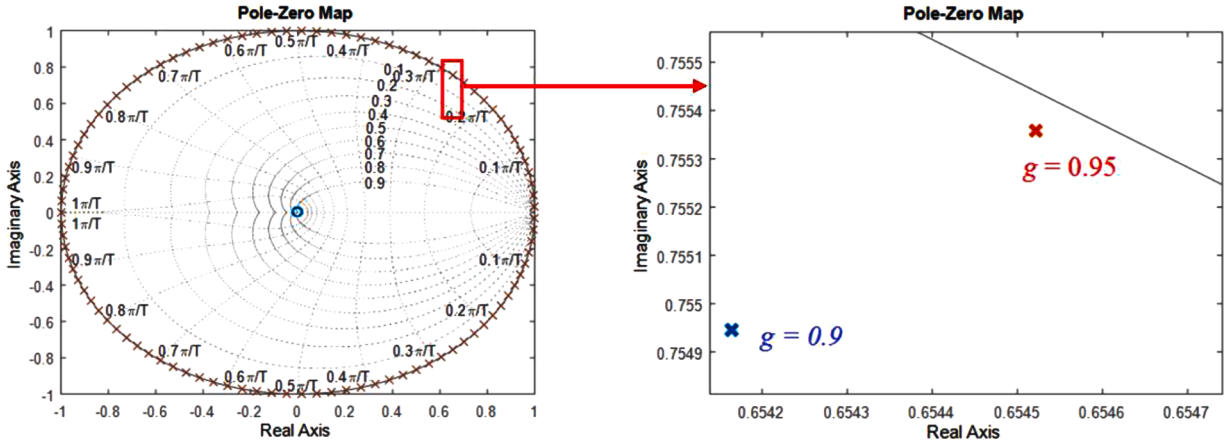

Fig. 2. Pole zero map of the feedback comb filter and its extended view for various *g* coefficient values (poles are inside the unity circle).

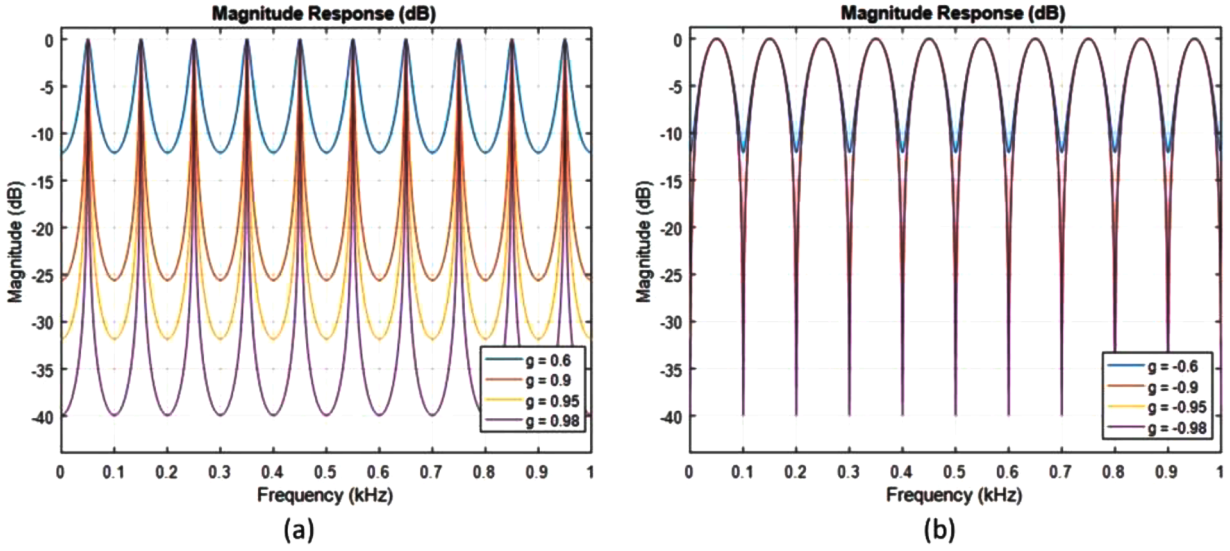

Fig. 3. Example of magnitude frequency characteristics of (a) feedback, (b) feedforward digital comb filter (both tuned at f_s = 9.9 kHz, M = 99) for various *g* values with normalization coefficient K_n included.

$$G_{PR}(z) = k_p + \frac{2k_r K_T \omega_c z^{-1} - 2k_r K_T \omega_c z^{-2})}{K_T^2 + 2K_T\omega_c + \omega^2 - (2K_T^2 - 2\omega^2)z^{-1} + (K_T^2 + 2K_T\omega_c + \omega^2)z^{-2}} = k_p + \frac{a_1 z^{-1} - a_2 z^{-2}}{b_0 - b_1 z^{-1} + b_2 z^{-2}} \quad (5)$$

$$G_f(z) = \sum_{k=0}^{N} b_k z^{-k} \quad (6)$$

where $K_T = 2/T_s$, ω – grid angular frequency, ω_c – bandwidth frequency.

The current error is processed by the PR and the comb filter harmonic compensator which has been tuned to provide resonant peaks at (2*n*-1) multiples of fundamental frequency which is considered constant. Hence, regardless of the comb type filter used, only odd harmonics are eliminated if it is designed as per dependencies outlined in (1)-(3). Because of that, the comb filter compensator acts also on the fundamental component, which can be treated as a support of the main PR controller. Compared to state-of-the-art multiple resonant harmonics compensation [9, 14, 26] the proposed in this paper structure is much simpler. It only utilizes a single filter that provides multiple harmonics control with simple digital notation and, if feedforward comb filter is used, FIR structure. On the other hand, individual harmonics cannot be controlled separately and adaptation to the varying system frequency is a challenge.

B. The comb filters properties for harmonics compensation in VOC control loop

The harmonic compensator output is tuned with constant gain K_{HC}, which should be adjusted according to harmonics contamination and stability constraints (this process is explained further in this section). Due to the fact that the feedback comb filter introduces poles to the system, its application is more critical from the stability viewpoint than utilization of the feedforward comb filter. However, by analogy to the repetitive control, it can be stated that in order to provide stability, two conditions have to be fulfilled, namely the closed loop poles of the main feedback plant controller as well as the comb filter should be within the unity circle (as demonstrated in Fig. 2) and the compensator should operate up to half of the Nyquist frequency [16, 20]. The first condition is fulfilled during the main controller design and the *g* coefficient. The second one is ensured by the presence of low-pass filter $G_f(z)$ with the cut-off frequency much lower than the Nyquist frequency. The feedforward comb filter structure does not introduce the poles to the system, therefore it complements the proportional portion of the main

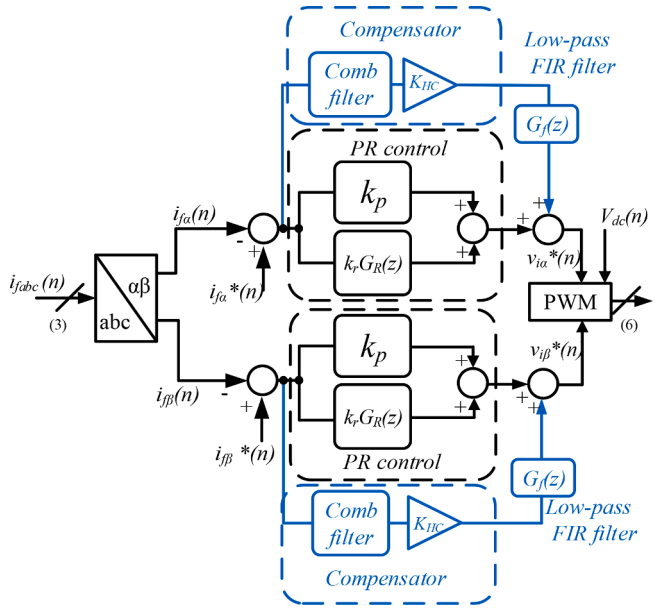

Fig. 4. VOC algorithm with proposed comb filters harmonic compensators.

controller. The controller design is shown in the next section.

For the purpose of this paper, a system with 9.9 kHz sampling frequency is used, hence the proposed cut-off frequency for filter $G_f(z)$ is 2.125 kHz. Furthermore, it should ensure the 2π phase shift at the resonant frequencies of the comb filter in order not to interfere with the comb filter output in its passband. Therefore the order of the series low-pass filter should, in this case, be equal to $N = 198$. Filter was designed with the equiripple method with the following parameters: passband ripple set to 0.001 dB (nearly flat passband) and stopband attenuation 80 dB. Any other method of FIR design can be used, as long as the resulting filter fulfils the requirements regarding the phase at the resonant peaks of the comb filter. The characteristics of this FIR filter cascaded with the comb filters is presented in Fig. 5.

As can be observed in both cases of comb filters the gain of resonant peaks can be controlled using K_{HC} parameter which is selected according to the procedure presented in the following section. The resulting compensator will act on odd order harmonics that are within a bandwidth of the series low pass FIR filter. With the low-pass FIR filter, the harmonics of order above a specified cut-off frequency will not be present in the harmonic compensator output, as can be seen in Fig. 5. In a similar concept of repetitive control, the robustness filters based on zero phase non-casual first order FIR low-pass filter or pure sample advance component and the series connection with main controller are typically used [19, 27, 28]. Unlike the one proposed here both above-mentioned filter types require information about the future sample which affects e.g. the tracking and/or disturbance rejecting capabilities [27].

C. The proposed procedure for design of a control loop

When it comes to the control loop gains design, it is a process that can be described as step-by-step as illustrated in Fig. 6. The controllers should be tuned according to the stability criteria which can be identified by means of bode plots that enable to determine the gain and phase margins (e.g. >~10dB and >~30 deg respectively).

Step 1 from Fig. 6 requires the plant model (PR design based on Bode plots of the open loop system will be used here). The resonant controller width frequency ω_c is assumed to be 0.5 rad/s. The plant transfer function (7) can be derived from the filter's parameters presented in Fig. 10 and discretized using the Tustin method with a sampling frequency of 9.9 kHz. The control design should account for a sample delay related to computational effort and measurement system time inertia.

$$G_p(s) = \frac{1}{R_f + (L_f + L_g)\cdot s} \tag{7}$$

where R_f - filter inductor resistance, L_f – filter reactor inductance, L_g – system inductance including coupling transformer ($L_g = 20$ μH).

Based on a Bode plot of the open-loop $G_{OL}(z)$ system (8) that also includes the delay $G_d(z)$ from Fig. 8 one can conclude that the designed gains k_p =6, k_r =30 provide a system stability with gain and phase margins equal to 18 dB and 66 degrees respectively [26]. The design was made using with initial estimates of k_p and k_r calculated as proposed in [9, 29–31].

$$G_{OL}(z) = G_p(z)\cdot G_d(z)\cdot\left[G_{PR}(z) + G_f(z)\cdot G_{FB}(z)\cdot K_{HC}\right] \tag{8}$$

As per step two, with the crossover frequency appearing at 2.5 kHz one can observe that the low-pass robustness FIR filter with 2.125 kHz cut-off frequency (i.e. 2 kHz pass-band edge frequency) presented in the proceeding section is sufficient for further design (Step 2).

The third step includes the choice of the comb filter type and damping factor that is a trade-off between selectivity and stability. In this paper, both feedback and feedforward filters are investigated. In

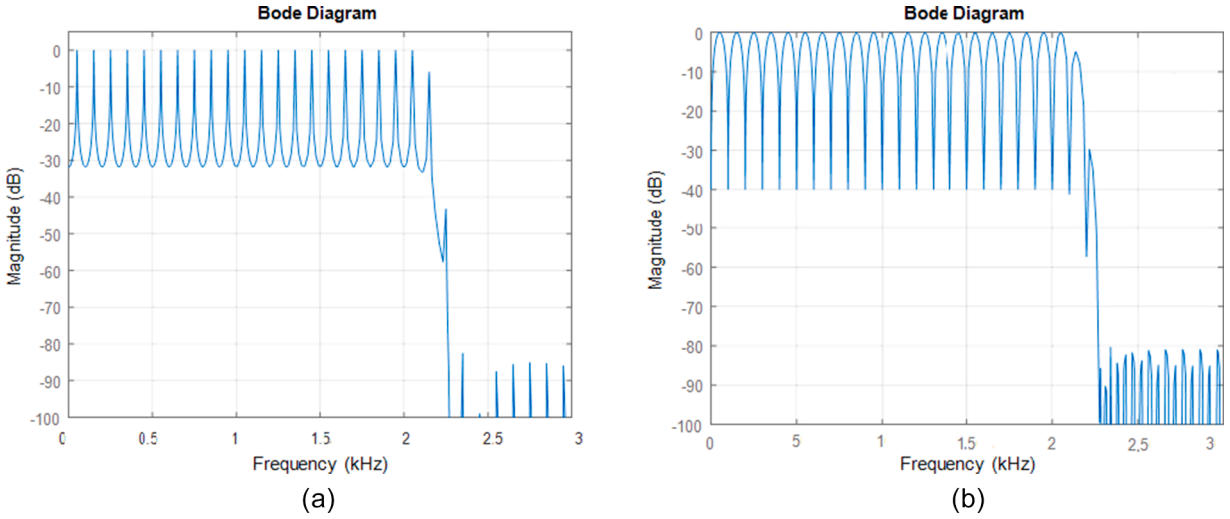

Fig. 5. Harmonic compensator (with low-pass FIR filter) normalized amplitude response (a) feedback comb filter based, with $g = 0.95$, (b) feedforward comb filter based, with $g = -0.98$.

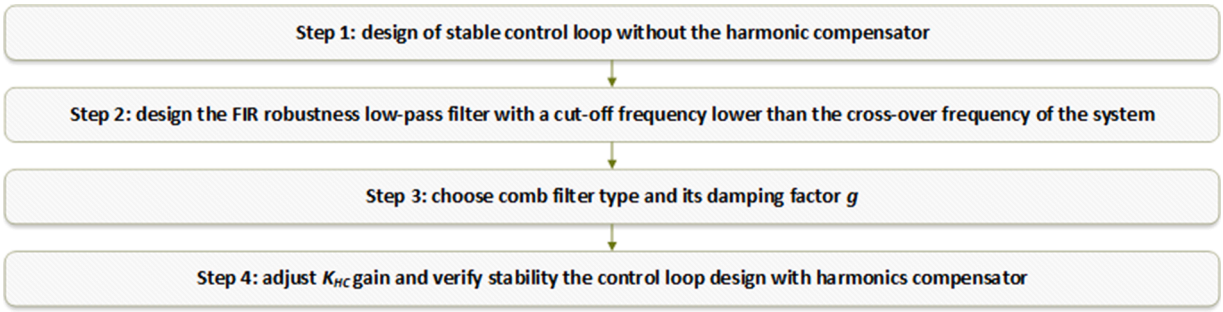

Fig. 6. Current control loop design step-by-step procedure for proposed harmonics compensation design.

general, the absolute value of g factor should be less than unity and depending on the filter structure ranging from 0.9 to 0.99. Higher values are proposed for feedforward comb filter whereas in case of feedback filter damping factor should be less or equal to 0.95 as depicted in Fig. 2. The damping coefficients of the comb filters used for this analysis are g = 0.95 for the feedback comb filter and g = -0.98 for the feedforward comb filter respectively.

Several IT tools were used during the research. First of all the developed algorithms were tested by means of numerical simulations and then adopted for code generation which can be uploaded on the dSPACE Real-Time Platform. The flow-chart explaining the workflow in the experimental implementation of the proposed control and synchronization algorithms is presented in Fig. 7.

The last step (Step 4) is tuning of the control loop with parallel comb filters. This can be easily done iteratively provides the stability of the system without the comb filters. As the compensator is connected in parallel it will provide additional amplification of the current error at certain frequencies. The feedback comb filter will be complementary to the resonant part and the feedforward comb filter to the proportional part. Therefore K_{HC} should be a fraction of the original gains. As a general remark based on this example it can be stated that if the designed gain margin of the main control loop is large enough, the K_{HC} should be within 0÷33% of k_r or k_p (depending on the required compensation type). Nonetheless, each time the harmonic compensator is added, the stability of the loop has to be verified. Based on the Bode plots shown in Figs. 9 and 10 the K_{HC} gain has been selected as follows: K_{HC} = 1 for feedforward comb filter and K_{HC} = 10 for feedback comb filter based compensators. The loop stability was preserved as per calculated gain and phase margins.

4. Study cases and description of the laboratory setup

The measurements for this paper were taken on the laboratory setup presented in Fig. 11. The 3 phase, two level converter coupled with the grid emulator via 3 phase transformer was controlled using dSPACE DS1006 platform. The PWM signals were delivered to the gate drivers via optic fiber cables in order to minimize delay and EMC problems. The converter was interfaced AC emulator which main component was programmable AC voltage source Chroma 61512 via a coupling transformer Yn/y and L filter. The two-level converter was based on IGBT power modules. It was supplied with a high power DC source EA-PSI 9750-40 for good stability of the DC link voltage V_{dc}. The grid voltage was reduced to V_{LLrms} =100 V at 50 Hz. The dSPACE provides the A/D converter range ± 5 V or ±15 V with 14 bits resolution. Voltage sensors LEM LV 25-P and current sensors LEM LA-125 P were used.

The measurements were performed under distorted supply voltage predefined harmonic spectrum as presented in Fig. 12 (V_{h5} = 3%, V_{h7} = 2.5%, V_{h11} = 3.5%, V_{h13} = 3%). The selection of the individual harmonics values was based on maximum values allowed in [32–34]. The resulting THD of the distorted voltage is 6.25% which is in line with international standards applicable for low-voltage systems [32–34]. The THD level specified by the IEEE in such case is 8% [32].

The active power set point was equal to 1.1 kW. Both the steady state performance and dynamic response of the compensator were considered. Both types of filters were compared on the basis of the resulting total harmonic distortion of the current.

5. Experimental results

All measurements were performed on the same voltage supply hence only the current output was depicted for each case. The THD (calculated up to 11 kHz to accordingly account for switching frequency distortion) of the current was calculated for each considered scenario i.e. with feedforward, feedback and without the comb filter compensation at all.

The first test case considered a control system based on PR controllers without additional harmonics compensation proposed by the Authors. The dominant distortion in the current comes from the valves switching as visible in Fig. 13. This is caused by fairly low filter inductance L_f = 1.2 mH (at tested power level) combined with a low switching frequency. Nonetheless, the effect of the distorted voltage is clearly reflected in the grid AC currents. The current THD, in this case, was 11.5%.

The operation of multiple harmonics compensation method based on the feedback comb is presented in Fig. 14. The current traces are significantly improved compared to the waveforms without compensation that are presented in Fig. 13. The low-order harmonics were efficiently minimised. This fact is also confirmed by the FFT spectrum,

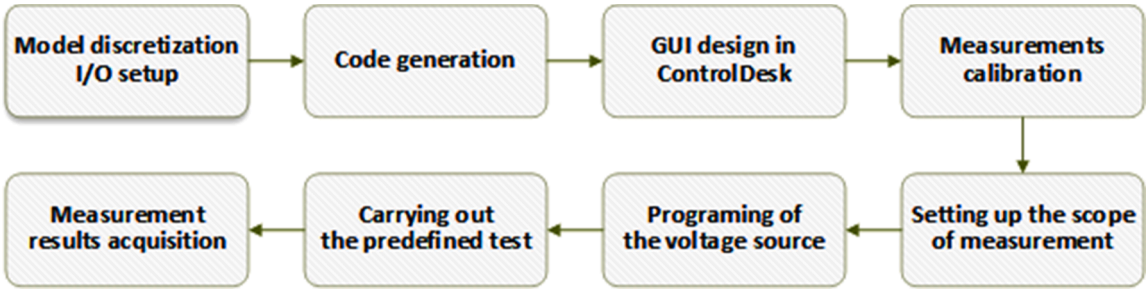

Fig. 7. Flow chart explaining conducted laboratory experiments.

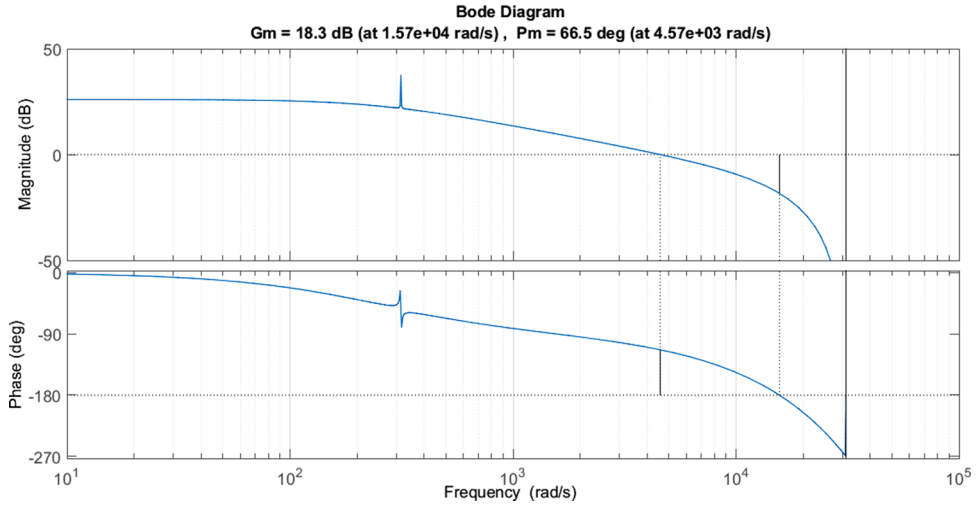

Fig. 8. Bode plot of main control without the harmonic compensator.

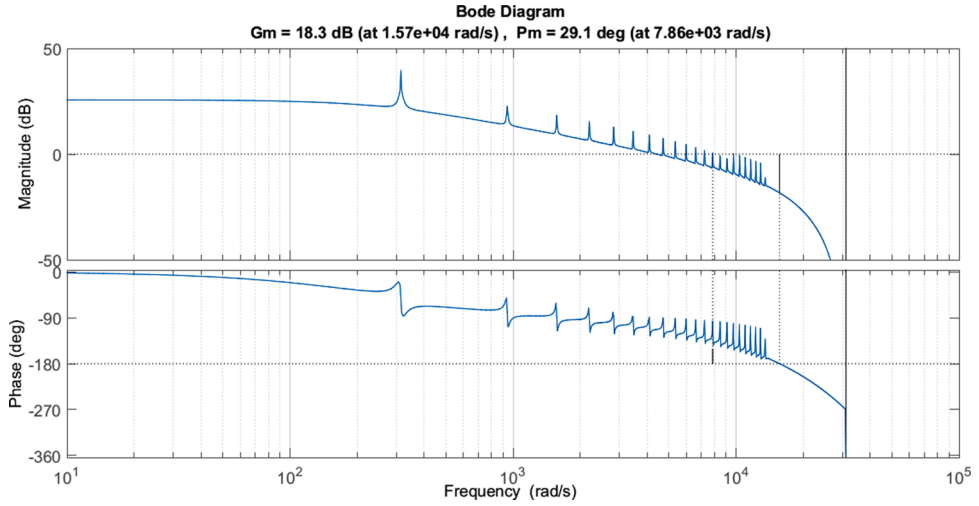

Fig. 9. Bode plot open loop of the system with compensator based on feedback comb filter $k_p = 6$, $k_r = 30$, $K_{HC} = 10$.

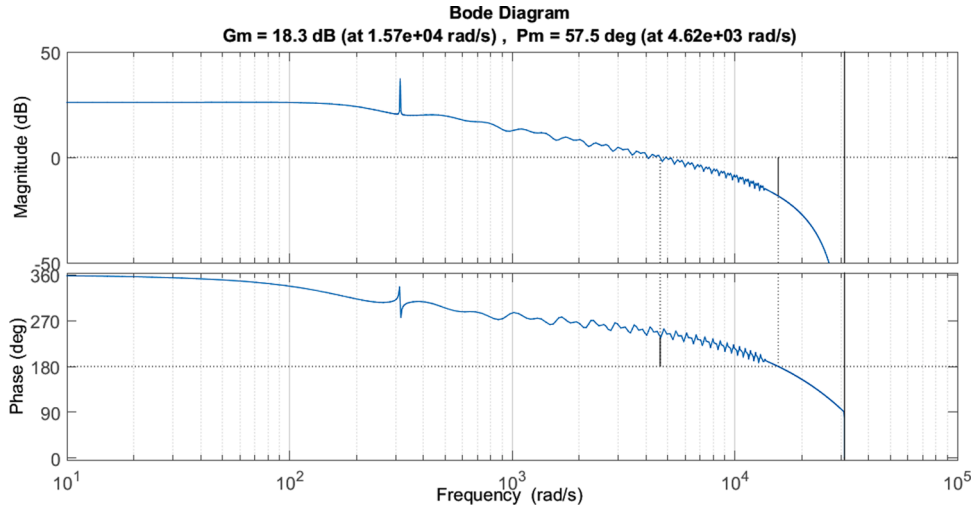

Fig. 10. Bode plot open loop of the system with compensator based on feedforward comb filter $k_p = 6$, $k_r = 30$, $K_{HC} = 1$.

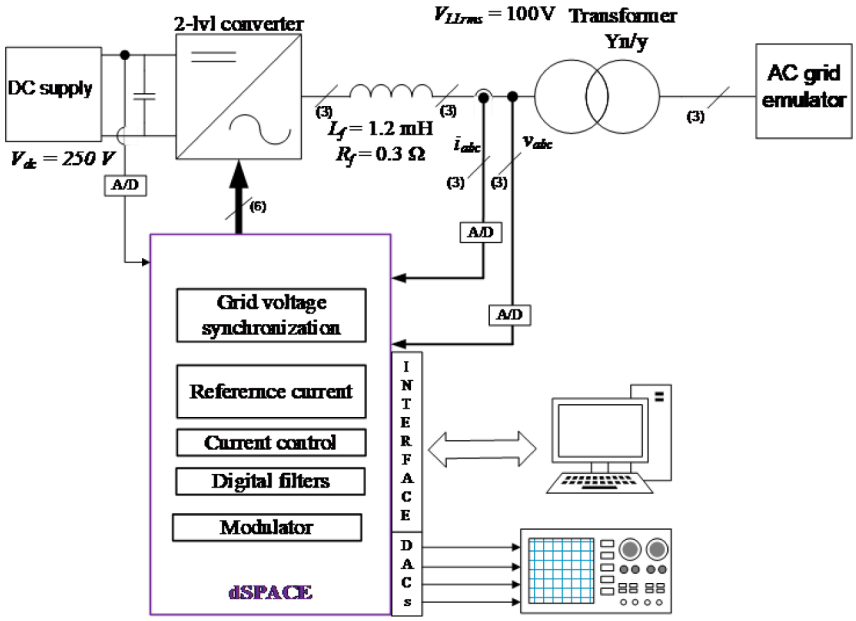

Fig. 11. Laboratory setup with the computer interface to the dSPACE platform for user control and measurements acquisition and high-accuracy oscilloscope Tektronix MSO 5034B for current traces recording.

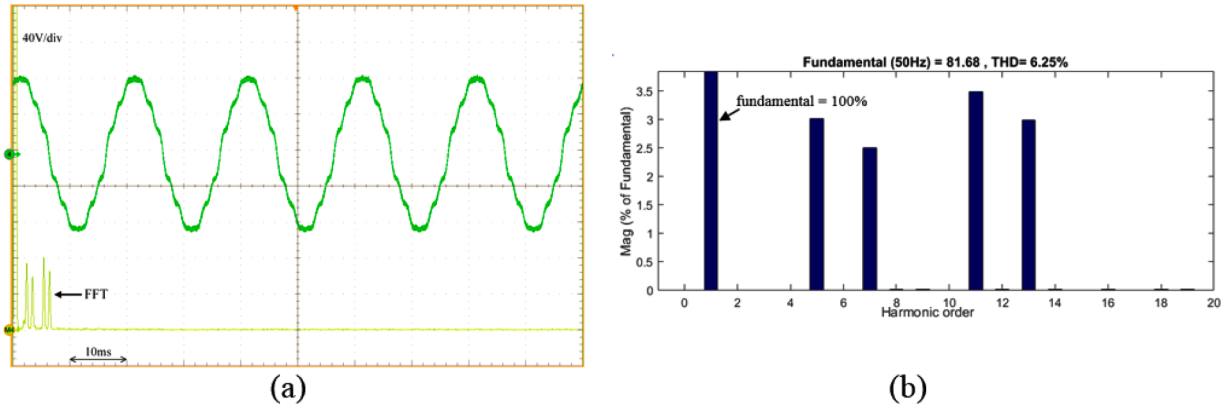

Fig. 12. Experimental results: (a) - supply voltage trace (only one phase shown, remaining two are the same in shape), (b) – FFT of the voltage.

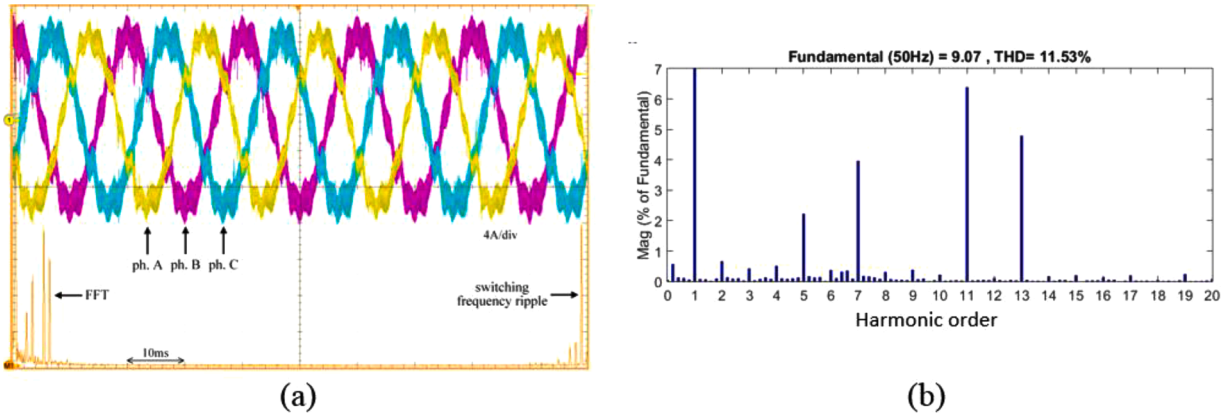

Fig. 13. Experimental results without harmonic compensation – converter current (a) and its FFT (b).

where harmonics (5th, 7th, 11th and 13th), are much lower than in the case with no compensation at all. In fact, all of these harmonic components are below 2.5 % which in the case of 11th and 13th harmonics means a reduction of approximately twice the time. This level of individual harmonics distortion complies with [35]. The THD of the output current decreased from 11.5 % to 7.5 % which accounts for 34%

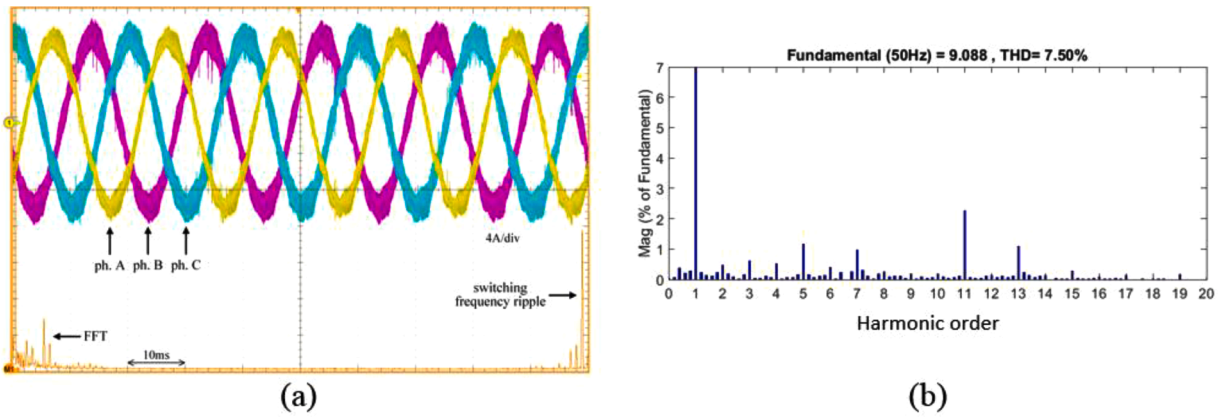

Fig. 14. Experimental results with feedback filter harmonic compensation - converter current (a) and its FFT (b).

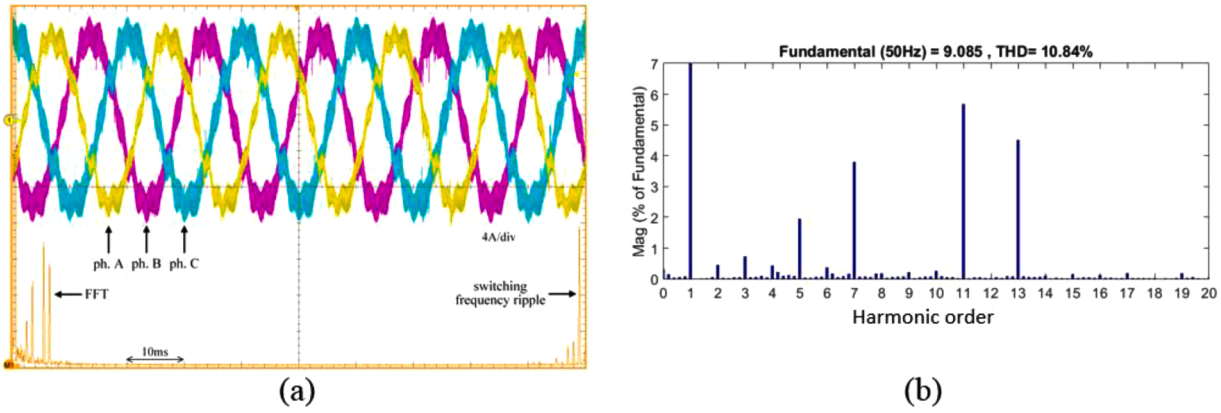

Fig. 15. Experimental results with feedforward filter harmonic compensation - converter current (a) and its FFT (b).

improvement

The feedforward comb filter based multiple harmonics compensator was proven to be not as effective. The current traces and the current FFT performed in Matlab for THD calculation are depicted in Fig. 15. The reduction of output current THD was 0.7 %, which accounts for around 6% proportional improvement. This is also visible in current traces as well as in current FFT. The smaller compensation level is caused mainly by the properties of the feedforward structure. Its frequency characteristic has much lower resonant peaks hence lower damping properties for current harmonics. However, the feedforward comb filter structure was still able to provide meaningful improvement.

As already mentioned in this paper the reasons for the range of THD in current was technical specifications of the laboratory setup and conservative assumptions for stability testing that are related mainly to

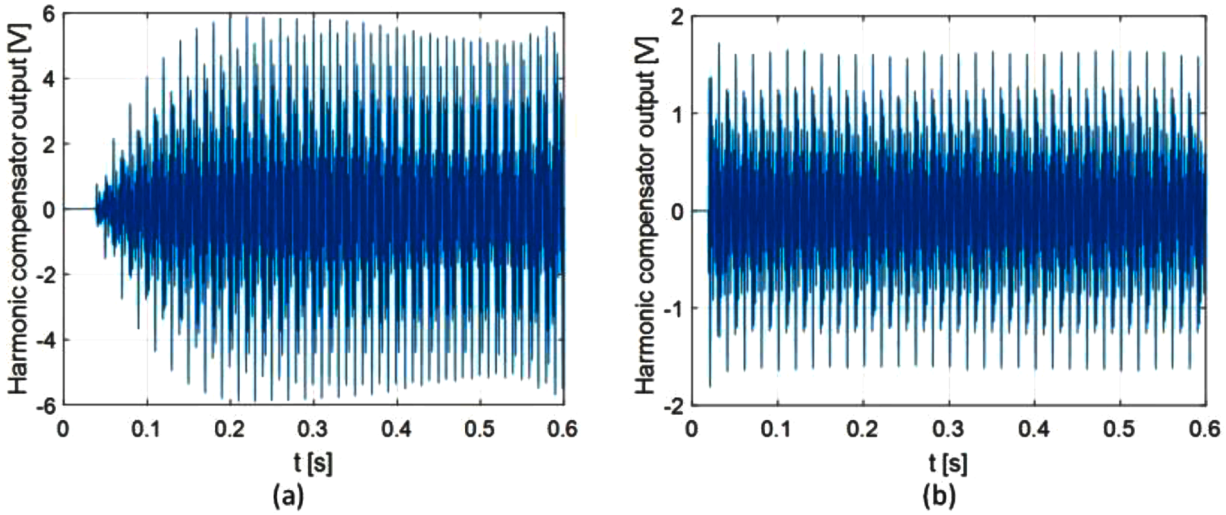

Fig. 16. Experimental dynamic response of harmonic compensation system when it is suddenly enabled – (a) –feedback filter harmonic compensation, (b) - feedforward filter harmonic compensation.

low switching frequency and the maximum permissible output power of the converter combined with fairly low filter inductance. As per IEEE 519™-2014 standard the THD limits in the current are dependent on the relation of inverter output current to the grid fault current (SCR ratio) [32]. Therefore, given the low output power of the inverter combined with much larger short-circuit current in LV networks, the obtained current distortion levels comply with the applicable IEEE and IEC standards [32, 35]. According to IEEE 519™-2014 standard the SCR ratio above 100 allow THD = 15% which is above what the authors obtained in the measurements with the proposed compensation. The SCR>100 for this study translates to approximately 650 A which can be considered a very low value [36, 37]. Therefore, these conditions can be considered conservative in terms of energy quality but also the stability assessment due to the switching frequency being fairly close to the harmonic compensator operating region.

Additionally, the dynamic performance of the proposed compensators can be investigated based on voltage trace and Short-Time Fourier Transform presented in Figs. 16 and 17. The output of the compensator has been measured once suddenly enabled in already running system. The feedback comb filter based compensator presents slower dynamics, but higher compensation signal amplitude. The feedforward comb filter based compensator is much faster, but at the same time has a lower compensation output compared to the feedback comb filter. This is caused by the filter's properties in the frequency domain visible in Fig. 3. Moreover, the time-frequency analysis indicates clearly that only the harmonics at the designed resonant frequencies are magnified. Hence, the compensation effect of the comb filter is confirmed.

The Table 1 below shows the summary of the proposed compensation performance during steady state operation.

Table 1
THD of current for proposed harmonics compensation - experimental results

Inverter output current THD	
Feedback comb filter harmonics compensation	7.5 %
Feedforward comb filter harmonics compensation	10.8%
No harmonics compensation	11.5 %

6. Influence of system frequency variations and performance discussion

The proposed structure of the compensator is most effective at the nominal grid frequency. As during the contingencies the grid frequency may vary, in such scenario the compensator may not be as effective, leading even to higher distortion than in no-compensation scenario. In order to keep the simplicity of the structure and minimize the impact of frequency variations, the authors propose to use a scaling gain K_{fvar} for the compensator. It is calculated based on grid frequency f measurement coming from e.g. PLL and frequency droop Δf selected close to expected maximum grid frequency variations (assumed positive).

$$K_{fvar} = \frac{\Delta f - |f_n - f|}{\Delta f} \tag{9}$$

Applying K_{fvar} as a multiplier for compensator can minimize or completely disable its operation when grid frequency variation reaches droop value. This prevents the over distortion of the current. Table 2 presents the simulation results for the system as in Figs. 4 and 10 with and without the K_{fvar} (8) included. The simulation does not include e.g. nonlinearities, communication delays, dead time etc. hence the distinct difference in quantitative results compared to the experiments, where much higher ripple was observed. Regardless, it can be observed that the selected droop value prevented current degradation largely above the level for no compensation scenario, even for high frequency variations. For the comparison of the performance of the proposed method with state-of-the-art compensation techniques, the multiple ideal resonant controllers tuned at 5th, 7th, 11th and 13th harmonics were investigated [26]. The gains for all the compensator components were tuned using the approach proposed in [38] and are respectively $k_{r5} = k_{r7} = 500$, $k_{r11} = k_{r13} = 3000$. The results, including comparison of computational burden, are presented in Table 3. As can be seen, the proposed feedback structure yielded similar effectiveness in THD reduction as the state-of-the-art method. Although computational burden calculated in the unit test for proposed compensator is slightly higher, it can be still considered moderate. This does not, however, impact the simplicity of design and digital implementation of the proposed solution compared to multiple resonant compensators where each gain has to be tuned

Table 2
Influence of grid frequency variations on THD of the current – simulation results

	$\Delta f = 2.1$ Hz $f = 50$ Hz	$f = 50.1$ Hz	$f = 52$ Hz
Feedback filter compensation without K_{fvar}	4.9%	6.3%	10.7%
Feedback filter compensation with K_{fvar}		6.7%	10.1%
Feedforward filter compensation without K_{fvar}	8.6%	9.0%	10.9%
Feedforward filter compensation with K_{fvar}		9.0%	10.3%
No compensation	10.2%		

Table 3
Comparison with other PR based harmonics compensation methods – simulation results

	THD of the inverter output current	Computational complexity
Feedback filter compensation	4.9%	0.4513 s
Feedforward filter compensation	8.6%	0.4513 s
Multi-resonant compensation	3.6%	0.42 s
No compensation	10.2%	n/a

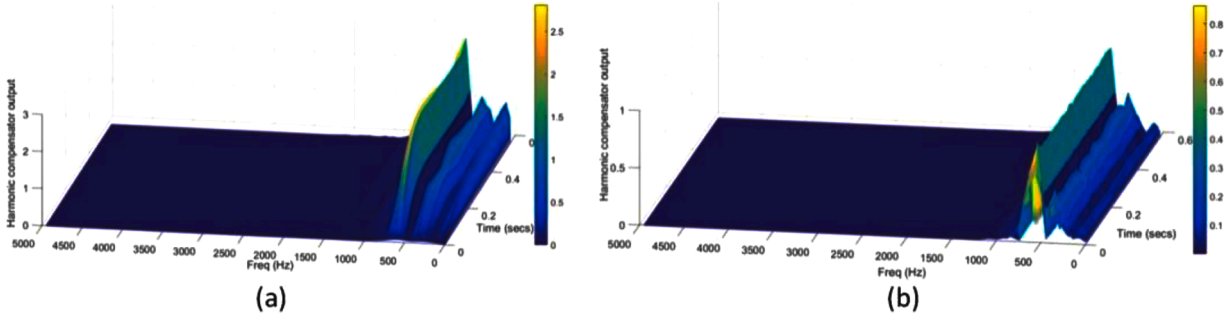

Fig. 17. Experimental Short-Time Fourier Transform of harmonic compensation output in volts – (a) –feedback filter harmonic compensation, (b) - feedforward filter harmonic compensation.

separately.

7. Conclusions

This paper proposes a modified approach to repetitive control based on comb filters for the multiple harmonics compensation in grid-connected converters. The proposed arrangement has been proven to be effective in the mitigation of higher harmonics present in the grid voltage by using just a single filter. The maximum proportional current THD reduction accounted for 34 % compared to the base scenario, where no compensation was present. Moreover, the conservative experimental assumptions confirmed the stability of the loop with the compensator and no interference with switching frequency was identified. With the plug-in structure, the compensator can be optionally enabled and tuned using the compensation gain. Compared to the classical harmonics compensation methods applicable to voltage oriented controlled converters, the proposed approach has simplified implementation and structure. The design procedure accounts for filter stability and is clear in the application. Furthermore, the notation in the discrete time domain facilitates the implementation of the real time systems using standard microcontrollers. Application of two types of comb filters is possible depending on the user needs. In the present case, one of the main drawbacks is the inability to obtain the operation of the comb filters when system frequency fluctuations are present. However, this question is addressed by the authors in another study.

Credits authors

Tomasz Chmielewski: Conceptualization, Methodology, Investigation, Software, Writing - Original Draft

Dariusz Zieliński.: Resources, Validation

Wojciech Jarzyna: Funding acquisition, Project administration, Supervision

Magdalena Chmielewska: Visualization, Writing - Reviewing and Editing,

K. Gopakumar : Validation

Declaration of Competing Interest

The authors declare that they have no known competing financial interests or personal relationships that could have appeared to influence the work reported in this paper.

Acknowledgements

This work was supported under the project "Electric vehicle energy transfer system integrated with lighting infrastructure – PLUGinEV" of the Polish National Centre for Research and Development, project No. POIR.04.01.02-00-0052/16.

References

[1] International Electrotechnical Commission, "Electromagnetic compatibility (EMC) Part 3-6: Limits — Assessment of emission limits for the connection of distorting installations to MV, HV and EHV power systems," IEC Standard, 2013.
[2] CIGRE Working Group 36-05, Harmonics characteristic parameters, methods of study, estimates of existing values in the network, Electra 77 (0) (1981) 35–54.
[3] IEEE, "IEEE Guide for Application of Power Electronics for Power Quality Improvement on Distribution Systems Rated 1 kV Through 38 kV," 2012.
[4] T. Chmielewski, Comb filters for harmonics control in grid connected power electronic converters applications Keywords Digital comb filter, in: Proceedings of the EPE 2017 - assigned jointly to the European Power Electronics and Drives Association & the Institute of Electrical and Electronics Engineers (IEEE), 2017.
[5] T. Chmielewski, Influence of Digital Filters In Voltage Oriented Control On The Operational Quality Of Grid-Tied Converters, Lublin University of Technology, 2018.
[6] T. Geyer, N. Oikonomou, G. Papafotiou, F.D. Kieferndorf, Model predictive pulse pattern control, IEEE Trans. Ind. Appl. 48 (2) (2012) 663–676.
[7] X. Zhao, et al., A voltage feedback based harmonic compensation strategy for current-controlled converters, IEEE Trans. Ind. Appl. 54 (3) (2017) 2616–2627.
[8] F. Blaabjerg, R. Teodorescu, M. Liserre, A.V Timbus, Overview of control and grid synchronization for distributed power generation systems, IEEE Trans. Ind. Electron. 53 (5) (2006) 1398–1409.
[9] M. Liserre, R. Teodorescu, F. Blaabjerg, Multiple harmonics control for three-phase grid converter systems with the use of PI-RES current controller in a rotating frame, IEEE Trans. Power Electron. 21 (3) (2006) 836–841.
[10] N.M. Dehkordi, N. Sadati, M. Hamzeh, A robust backstepping high-order sliding mode control strategy for grid-connected DG units with harmonic/interharmonic current compensation capability, IEEE Trans. Sustain. Energy 8 (2) (2016) 561–572.
[11] Y. Han, P. Shen, X. Zhao, J.M. Guerrero, An enhanced power sharing scheme for voltage unbalance and harmonics compensation in an islanded AC microgrid, IEEE Trans. Energy Convers. 31 (3) (2016) 1037–1050.
[12] D.K. Yoo, L. Wang, E. Rogers, Model predictive resonant control of a three-phase voltage source converter with selective harmonic compensation, in: Proceedings of the IEEE 24th International Symposium on Industrial Electronics (ISIE), 2015, pp. 1480–1485.
[13] R. Teodorescu, M. Liserre, P. Rodriguez, Grid Converters For Photovoltaic And Wind Power Systems, 29, John Wiley & Sons, 2011.
[14] T. Orłowska-Kowalska, F. Blaabjerg, J. Rodr'iguez, Advanced and Intelligent Control In Power Electronics And Drives, 531, Springer, 2014.
[15] W. Lu, K. Zhou, D. Wang, M. Cheng, A general parallel structure repetitive control scheme for multiphase DC–AC PWM converters, IEEE Trans. Power Electron. 28 (8) (2012) 3980–3987.
[16] Y. Yang, K. Zhou, H. Wang, F. Blaabjerg, D. Wang, B. Zhang, Frequency adaptive selective harmonic control for grid-connected inverters, IEEE Trans. Power Electron. 30 (7) (2014) 3912–3924.
[17] S. Hara, Y. Yamamoto, T. Omata, M. Nakano, Repetitive control system: A new type servo system for periodic exogenous signals, IEEE Trans. Autom. Control 33 (7) (1988) 659–668.
[18] R. Costa-Castelló, R. Grinó, E. Fossas, Odd-harmonic digital repetitive control of a single-phase current active filter, IEEE Trans. Power Electron. 19 (4) (2004) 1060–1068.
[19] Q. Zhao, Y. Ye, G. Xu, M. Zhu, Improved repetitive control scheme for grid-connected inverter with frequency adaptation, IET Power Electron. 9 (5) (2016) 883–890.
[20] A. Lidozzi, C. Ji, L. Solero, P. Zanchetta, F. Crescimbini, Resonant–repetitive combined control for stand-alone power supply units, IEEE Trans. Ind. Appl. 51 (6) (2015) 4653–4663.
[21] R. Nazir, K. Zhou, N. Watson, A. Wood, Analysis and synthesis of fractional order repetitive control for power converters, Electr. Power Syst. Res. 124 (2015) 110–119.
[22] A.R. Monter, E.J. Bueno, A. García-Cerrada, F.J. Rodríguez, F.M. Sánchez, Detailed analysis of the implementation of frequency-adaptive resonant and repetitive current controllers for grid-connected converters, Electr. Power Syst. Res. 116 (2014) 231–242.
[23] H. Liu, Y. Xing, H. Hu, Enhanced frequency-locked loop with a comb filter under adverse grid conditions, IEEE Trans. Power Electron. 31 (12) (2016) 8046–8051.
[24] H. Liu, H. Hu, H. Chen, L. Zhang, Y. Xing, Fast and flexible selective harmonic extraction methods based on the generalized discrete Fourier transform, IEEE Trans. Power Electron. 33 (4) (2017) 3484–3496.
[25] C. Xie, K. Li, J. Zou, K. Zhou, J.M. Guerrero, Multiple second-order generalized integrators based comb filter for fast selective harmonic extraction, in: Proceedings of the IEEE Applied Power Electronics Conference and Exposition (APEC), 2019, pp. 2427–2432.
[26] R. Teodorescu, F. Blaabjerg, M. Liserre, P.C. Loh, Proportional-resonant controllers and filters for grid-connected voltage-source converters, IEE Proc. Electric Power Appl. 153 (5) (2006) 750–762.
[27] A. Lidozzi, C. Ji, L. Solero, F. Crescimbini, P. Zanchetta, Load-adaptive zero-phase-shift direct repetitive control for stand-alone four-leg VSI, IEEE Trans. Ind. Appl. 52 (6) (2016) 4899–4908.
[28] R. Nazir, K. Zhou, N.R. Watson, A. Wood, Frequency adaptive repetitive control of grid-connected inverters, in: Proceedings of the International Conference on Control, Decision and Information Technologies (CoDIT), 2014, pp. 584–588.
[29] P. Antoniewicz, "Predictive control of three phase AC/DC converters," The Institute of Control and Industrial Electronics, 2009.
[30] M. Malinowski, "Sensorless control strategies for three-phase PWM rectifiers," Warsaw University of Technology, 2001.
[31] M. Malinowski, S. Stynski, W. Kolomyjski, M.P. Kazmierkowski, Control of three-level PWM converter applied to variable-speed-type turbines, IEEE Trans. Ind. Electron. 56 (1) (2008) 69–77.
[32] IEEE Recommended Practice and Requirements for Harmonic Control in Electric Power Systems, IEEE Std (2014) 1–29. *519-2014 (Revision of IEEE Std 519-1992)*.
[33] "EN 50160, Voltage characteristics of electricity supplied by public electricity networks," pp. 1–34, 2010.
[34] "IEC 61000-2-2:2002 Electromagnetic compatibility (EMC) - Part 2-2: Environment - Compatibility levels for low-frequency conducted disturbances and signalling in public low-voltage power supply systems," pp. 1-, 2002.
[35] "IEC 61000-3-2:2018 Electromagnetic compatibility (EMC) - Part 3-2: Limits - Limits for harmonic current emissions (equipment input current ≤16 A per phase)," pp. 1–73, 2018.

[36] "IEC 60076-5:2006 Power transformers - Part 5: Ability to withstand short circuit," pp. 1–71, 2006.
[37] J.J. Burke, D.J. Lawre, Characteristics of Fault Currents on Distribution Systems, IEEE Trans. Power Apparat. Syst. PAS-103 (1) (1984) 1–6.
[38] D. De, V. Ramanarayanan, A Proportional + Multiresonant Controller for Three-Phase Four-Wire High-Frequency Link Inverter, IEEE Trans. Power Electron. 25 (4) (2010) 899–906.